Original Article

High Performance Polymers

High Performance Polymers
2022, Vol. 34(8) 904–913

DOI: 10.1177/09540083221097381
journals.sagepub.com/home/hip
SAGE

Synthesis and characterization of adamantane-based copolyimides with high transparency

Qi Li[1], Sung S Park[2], Chang-Sik Ha[2], Shuai Yuan[1,3] and Liyi Shi[1,3]

Abstract

In this work, a copolyimide (Co-PI) film with high transparency was prepared by the copolymerization of hexafluoroisopropylidene)diphthalic anhydride (6FDA), 3,3′,4,4′-biphenyltetracarboxylic dianhydride (BPDA), 2,2′-Bis(trifluoromethyl)benzidine (TFMB) and adamantane-1,3-diamine (DAA). The effects of DAA monomers on the optical, thermal, and mechanical properties of the co-PIs were discussed in detail. We found that the preparation of polyimide (PI) based on the combination of two dianhydrides and two diamines could obtain the co-PI film with excellent comprehensive performance due to the synergy between the -CF_3 group, the aliphatic ring and the aromatic structure. Through the structure and composition optimization, the co-PI film with 1.30% DAA (Q3) has a T_g of 374°C, T_5 higher than 530°C, T_{430} of 82% and the tensile strength higher than 145 MPa. These results indicate that the Co-PI films can be successfully utilized in the development of novel heat-resistant plastic substrates for the optoelectronic engineering applications.

Keywords

Transparent, co-polyimide, adamantane, structure-properties relationship

Introduction

Polyimides (PIs) are one kind of high performance polymers with outstanding thermal stability, excellent low temperature stability, good mechanical properties, dimensional stability, dielectric and insulation properties, good radiation resistance, chemical stability and flame retardancy due to a large number of nitrogen-containing five-membered heterocyclic and aromatic rings and the conjugation effect among these rings, which make them suitable for applications in many high-tech fields, such as automotive, electronics, and aerospace industry.[1–8] However, aromatic PI films generally suffer from the yellow or dark brown color and exhibit a poor optical transmittance originated from the formation of charge transfer complexes (CTC) between the electron donor diamine and the electron acceptor dianhydride in the main backbone,[9–11] which is one of the great disadvantages for microelectronics and optoelectronic applications. In recent years, with the increasing demands for high reliability, high integration, and high signal transmission speed in optoelectronic devices, high thermal stability and high dimensional stability at elevated temperatures are also considered as key performance indicators for PI films used as flexible substrates.

The optical transparency of PI can be improved by introducing fluorine-containing substituents, such as trifluoromethyl, hexafluoroisopropyl or perfluoro groups,[12–16] flexible linkages,[17–21] aliphatic/alicyclic structure,[22–26] unsymmetrical units,[27,28] meta-substituted structure,[29,30] bulky pendent groups[31–33] or non-coplanar structure[34,35] in polyimide chains. Among these strategies, introducing fluorinated and alicyclic structure is two effective ways for synthesizing transparent polyimide.[36,37] However, fluorinated aromatic PIs still remain to have weak coloration in the visible region attributed to the presence of charge transfer (CT) interactions caused by the aromatic backbones. The bulky fluorine-

[1]Emerging Industries Institute, Shanghai University, Jiaxing, China
[2]Department of Polymer Science and Engineering, School of Chemical Engineering, Pusan National University, Busan, Republic of Korea
[3]Research Centre of Nanoscience and Nanotechnology, Shanghai University, Shanghai, China

Corresponding authors:
Shuai Yuan, Research Centre of Nanoscience and Nanotechnology, Shanghai University, 99 Shangda Road, Shanghai 200444, China.
Email: s.yuan@shu.edu.cn

Liyi Shi, Research Centre of Nanoscience and Nanotechnology, Shanghai University, 99 Shangda Road, Shanghai 200444, China.
Email: shiliyi@shu.edu.cn

containing substituents can also increase the free volume of polyimide and disrupt the coplanarity and linearity of molecular chains so that there is a danger that the coefficient of thermal expansion (CTE) is markedly increased.[38,39] Compared with aromatic PIs, PIs with aliphatic/alicyclic structure always display higher transparency originated from their relatively low probability of undergoing inter- or intramolecular CT interaction. The incorporated aliphatic/alicyclic segments to some extent deteriorates PI thermal stability, which is reflected as long-term heat resistance such as nonflammability and thermo-oxidative stability and short-term heat resistance such as the glass transition temperature (T_g). However, it is worth noting that the introduction of rigid polycyclic group such as adamantane directly or as a pendent group into the polymer backbone can induce high T_g and low CTE values, but the long-term heat resistance is still poor due to the nature of the alicyclic ring.[40–46] Thus, combining adamantane with fluorinated groups and aromatic structures is an effective way to achieve copolymerized PI (Co-PI) films with desired optical transparency, thermal stability and dimensional stability.

In this work, we used 4,4′-(hexafluoroisopropylidene) diphthalic anhydride (6FDA) and 3,3′,4,4′-biphenyltetracarboxylic dianhydride (BPDA) as dianhydride monomers, and 2,2′-bis(trifluoromethyl)benzidine (TFMB) and an alicyclic diamine, adamantane-1,3-diamine (DAA) as diamine monomers to prepare PI films by a quaternary copolymerization. The charge transfer in PI backbone was reduced by alicyclic and hexafluorine moieties for optical transparence. In addition, introducing the stiff alicyclic diamine (DAA) and rigid aromatic dianhydride (BPDA) further improved the thermal stability, mechanical properties, and dimensional stability. The copolymerization approach is easy to maintain the high transparency of the PI film without sacrificing many advantages of traditional aromatic polyimides, such as thermal stability and dimensional stability. We adjusted the ratio of diamine monomers to achieve balanced distribution of rigid structures and flexible structures, aromatic structures and aliphatic ring structures in the PI chains, and the optical properties, thermal stability and dimensional stability of the random Co-PI films were investigated in detail.

Experimental section

Materials

4,4′-(Hexafluoroisopropylidene)diphthalic anhydride (6FDA, 99%), and 3,3′,4,4′-Biphenyltetracarboxylic dianhydride (BPDA, 99%) were obtained from J&K Chemical Ltd. (Beijing, China). 2.2'-Bis(trifluoromethyl)benzidine (TFMB, 98%) was purchased from Shanghai Macklin Biochemical Co., Ltd. Adamantane-1,3-diamine (DAA, > 98%) was supplied by Tokyo Chemical Industry Co., Ltd. N,N-Dimethylacetamide (DMAc, anhydrous grade, 99.8%) was obtained from from Aladdin Reagent Co., Ltd. (Shanghai, China). All of the above regents were used without further purification

Preparation of Co-PI films

Co-PIs were synthesized by a conventional two-step method via poly(amic acid)s (PAAs), and the monomer content ratios of the Co-PIs prepared in this study are given in Table 1. A representative example for the synthesis of Q4 is described here. Firstly, 18.5 mmol TFMB and 1.5 mmol DAA were added in a 100 mL vial, and then the mixture was dissolved in 41.68 g DMAc. After that, 4 mmol 6FDA and 16 mmol BPDA were added successively to the above solution, and an additional volume of DMAc (15 g for each) was added to wash the residual dianhydride, and the solid content of the reaction system was adjusted to be 15%. The mixture was stirred at room temperature for 24 h to yield a viscous PAA solution.

The PAA solution was cast onto clean glass plates, and the solvent was evaporated at 60°C for 4 h. After that, the PAA film was imidized on the glass plate by sequential heating at 120, 180, 250, and 300°C for 1 h each in an inert atmosphere oven which allows the oxygen level to be maintained at 50 ppm or less. After cooling down, the Co-PI film was peeled off from the glass substrate by immersion in tap water for a few minutes. The thickness of Co-PI film was controlled to be approximately 50 μm.

Characterization

Attenuated total reflection (ATR) Fourier transform infrared (FTIR) spectra were obtained with 32 scans per spectrum at a resolution of 2 cm^{-1} using a Nicolet Thermofisher IS50. Inherent viscosity (η_{int}) was determined on an Ubblohde viscometer in thermostatic container with the PAA concentration of 0.5 g/dL in DMAc at 25°C. Wide angle X-ray diffractometry (XRD) measurements were performed by a Shimadzu XRD-6100 X-ray diffractometer using Cu/Kα radiation (λ = 1.54 Å) at room temperature. Data were collected at 0.02° intervals over the range of 5–80°, and the scan speed was 0.5° (2θ)/min.

UV-visible optical transmission spectra of the Co-PI films were measured using a Shimadzu UV-1650 PC spectrometer in the wavelength range 200–800 nm with a resolution of 0.5 nm and a scanning rate of 200 nm/min. Thermal decomposition behavior of the Co-PI films was observed using a Perkin-Elmer TGA 4000 at a heating rate of 10°C/min from 30 to 800°C under a nitrogen atmosphere. Dynamic mechanical analysis (DMA) was done by using a Q800 (TA Instruments) operating in tensile mode at a constant frequency of 1 Hz along with a

Table 1. Molar feed ratios used in the Co-PI synthesis.

Co-PI	6FDA/mmol	BPDA/mmol	TFMB/mmol	DAA/mmol	DAA/(wt%)[a]	η_{int}/(dL/g)	Film quality
Q0	4	16	20	0	0	0.61	Flexible
Q1	4	16	19.8	0.2	0.26	0.59	Flexible
Q2	4	16	19.5	0.5	0.65	0.54	Flexible
Q3	4	16	19	1	1.30	0.53	Flexible
Q4	4	16	18.5	1.5	1.97	0.53	Flexible
Q5	4	16	18	2	2.64	0.50	Brittle

[a]The weight percent of DAA is based on the total weight of the dianhydride and diamine monomers.

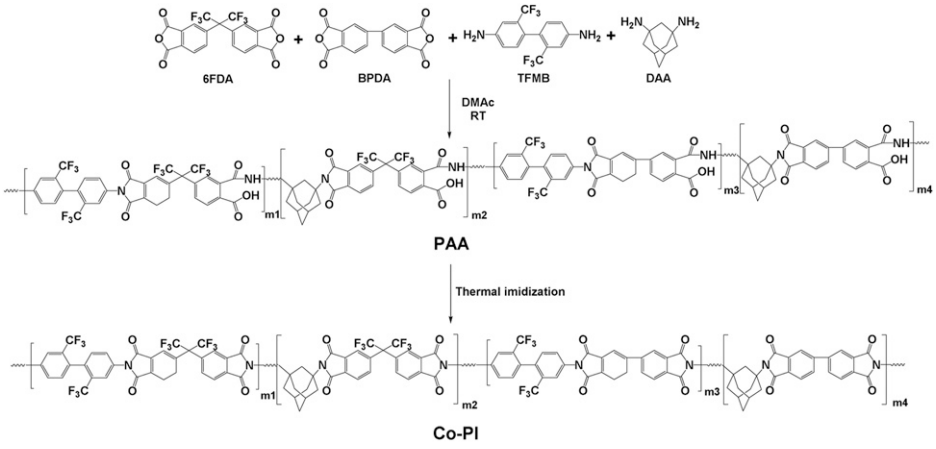

Scheme 1. Synthetic route of Co-PI films.

load of 0.1 N. The characterization was performed over a temperature range from 50 to 400°C with a heating rate of 3°C/min. Differential scanning calorimetric (DSC) analysis were conducted with a Mettler Toledo DSC 1 with a heating rate of 10°C/min in nitrogen purge. The coefficients of thermal expansion (CTE) of the samples were measured by a Mettler Toledo TMA/SDTA840 thermomechanical analyzer (Zurich, Switzerland), which was used to apply an expansion force of 0.1 N to the films at a heating rate of 5°C/min in the temperature range 30–350°C.

The tensile strength, Young's modulus, and elongation at break were measured by using a universal testing machine (MTS systems Co., Ltd., China) at a crosshead speed of 5 mm/min with 4 mm width for all the samples. Stress-strain measurements were performed on dumbbell-shaped samples cut from the films according to GB/T 1040.3–2006. At least five identical specimens were tested for each sample, and their average mechanical properties were reported.

The water absorption of the films (10 mm × 10 mm × 0.5 mm) was measured by immersion of preweighed dry films in DI water for 24 h at room temperature. After the excess water was wiped from the film surface by using filter paper, the weight of the swollen film was measured immediately. The water absorption was expressed as the weight percentage of water in the swollen sample as:

$$\text{Water absorption} = \frac{(m_2 - m_1)}{m_1} \times 100\% \quad (1)$$

where m_1 is the weight of the dry sample and m_2 is the weight of the swollen sample.

For the determination of solubility, 10 mg of polyimide resin was dissolved in 1 mL organic solvent to observe the dissolving state of polymer at room temperature (RT) and heating conditions. The solubility was determined visually as four grades: completely soluble (+), partially soluble (±), swelling (Δ), and insoluble (−).

Results and discussion

Preparation and characterization of Co-PI films

As shown in Scheme 1, a series of Co-PI films were synthesized via a two-step procedure with poly (amic acid) (PAA) as precursors, followed by thermal imidization at elevated temperature to 300°C. As shown in Table 1, the inherent viscosities (η_{int}) of the intermediate PAA precursors range from 0.50 to 0.61 dL/g, and the high viscosities provide

the possibility for the subsequent film-forming.[47] The viscosity decreases monotonically as the DAA content in the polymer chains increases. This is probably because that the bulky rigid adamantane group in the DAA monomer restricts the growth of molecular weight of Co-PI.[48,49] The formation of Co-PI films is confirmed with FTIR spectra. Figure 1(a) demonstrates the IR spectra of Co-PI Q0-Q5. All the samples exhibit characteristic imide group absorptions around 1780 and 1720 cm^{-1} (typical of imide carbonyl asymmetrical and symmetrical stretch), 1360 cm^{-1} (C-N stretch), and 736 cm^{-1} (imide ring deformation). The absorptions due to C-F stretching in $-CF_3$ and unsaturated C-H stretching in phenyl are also observed at about 1120 cm^{-1}[50,51] and 3080 cm^{-1},[52] respectively. The absorption peak at 1618 cm^{-1} is associated to the stretching vibration of 1,4-C_6H_4 in backbone.[53] There is no existence of the characteristic absorption bands of the amide at 3200 and 1520 cm^{-1}, which indicates the complete imidization reaction of Co-PI films. Compared with curve Q0, the characteristic absorptions at 2919 cm^{-1} and 2868 cm^{-1} assigned to the C-H stretching vibration of the adamantyl group[54,55] appear in the curves of Q1-Q5. As TFMB is progressively replaced by DAA, the peak intensity of the above C-H stretching vibration of the adamantyl group (Figure 1(b)) becomes stronger, while the peak intensity at 1618 cm^{-1} (Figure 1(c)) decreases obviously. The FTIR results further indicates that DAA had been successfully introduced into the molecular chain of Co-PI.

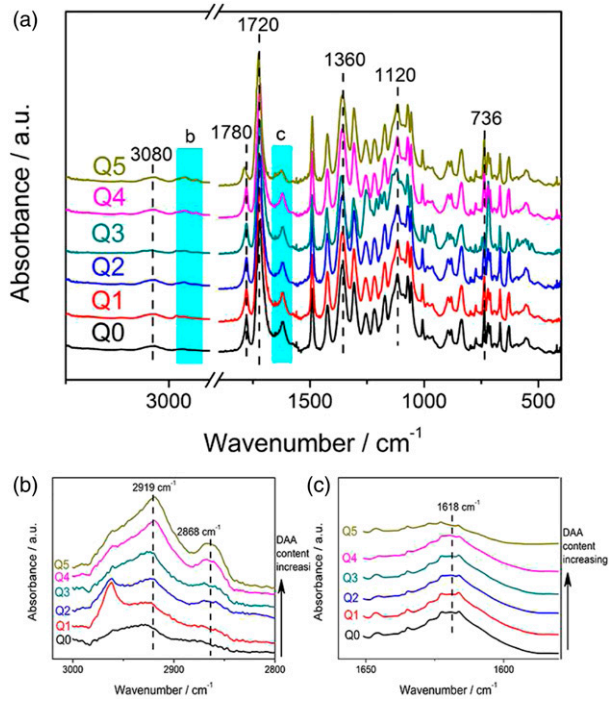

Figure 1. (a) FTIR spectra of Co-PI films; (b) C-H stretching vibration of the adamantyl group; (c) C-C stretching vibration of 1,4-C_6H_4 in backbone.

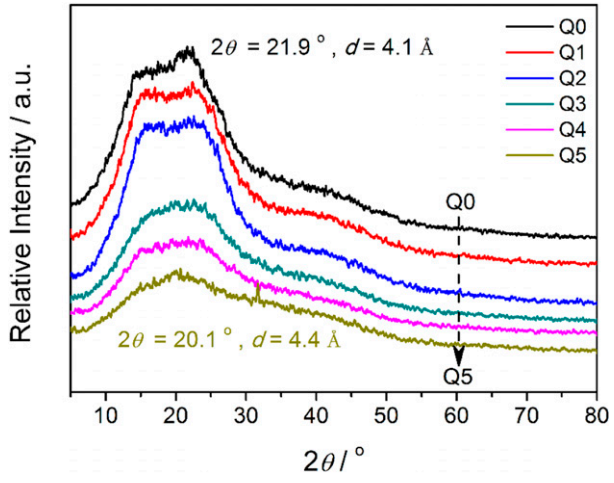

Figure 2. XRD patterns of Co-PI films.

Morphology study of Co-PI films

The aggregation structures of the obtained Co-PIs were investigated by XRD study. XRD patterns of Co-PIs are illustrated in Figure 2. There is no crystallization feature as observed from the broad diffraction peaks, indicating that all of the Co-PIs showed an amorphous structure in matrix. This result reveals that the linearity and rigidity of PI chains could be disturbed by the steric hindrance of bulky trifluoromethyl and adamantane substitutes. The mean inter-chain distance (d) values are calculated using the scattering angle (2θ) from the Bragg's equation ($n\lambda = 2d \sin \theta$)[56–58] and are used to quantitatively present the packing of molecular chains. It is noticeable that Q0 showed small d value of 4.1 Å, whereas Q5 exhibited the largest d value up to 4.4 Å. A larger d value indicates less close chain packing. The d value increases with increasing DAA unit content. The result can be attributed to the bulky structure of DAA, which leads to irregularity and bulkiness of the polyimide chains, finally resulting in effective disturbance of the chain packing and increased inter-chain distance.[59,60]

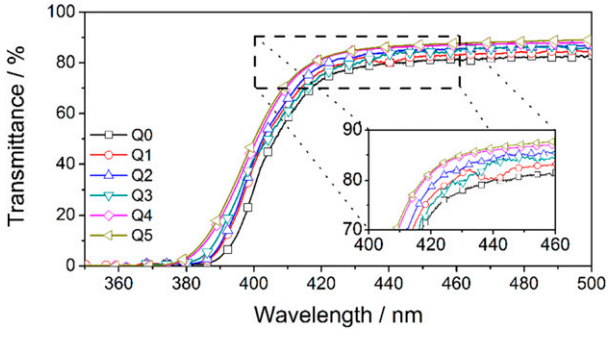

Figure 3. UV-vis spectra of Co-PI films with various contents of DAA.

Optical properties of Co-PI films

The optical properties of the Co-PI films with various diamine monomer ratios were determined by UV-visible measurement. Figure 3 depicts the UV-Vis spectra of the Co-PI films with a thickness of 50 μm. The optical transparency obtained from the UV-vis spectra, including cut-off wavelength (λ_0) and transmittance at 430, 450, and 500 nm, are summarized in Table 2. The fluorinated Q0 film showed good transparency with a low λ_0 value of 385.7 nm and optical transmittance about 78% at 430 nm. As the DAA loading increased, the transmittance at 430 nm of the Co-PI films (Q1-Q5) increased from 79.6% for Q1 to 85.1% for Q5 and the λ_0 value exhibited an obvious blue shift from 382.1 nm for Q1 to 376.0 nm for Q5, indicating that the use of bulky alicyclic DAA is more beneficial for the increase of transparency compared with fluorinated aromatic TFMB due to more effectivity to eliminate CTC formation between polymer chains through steric hindrance and weak electron-donating properties. The results demonstrated that the copolymerization of 6FDA, BPDA, TFMB, and DAA is an effective way to prepare the colorless and transparent PI films. As a result, these Co-PI films can be used in organic light emitting diode (OLED) devices which require a substrate material with a light transmission of more than 80% at 430 nm.[61]

Table 2. Optical properties of Co-PI films.

Co-PI	λ_0[a]/nm	T_{430}[b]/%	T_{450}[b]/%	T_{500}[b]/%
Q0	385.7	78.0	80.9	82.9
Q1	382.1	79.6	82.5	84.6
Q2	382.2	81.5	85.1	86.7
Q3	378.6	82.3	84.5	86.9
Q4	377.0	84.8	86.6	88.0
Q5	376.0	85.1	87.2	89.2

[a]λ_0: UV cut-off wavelength.
[b]T_{430}, T_{450}, T_{500}: transmittance at 430, 450 and 500 nm, respectively.

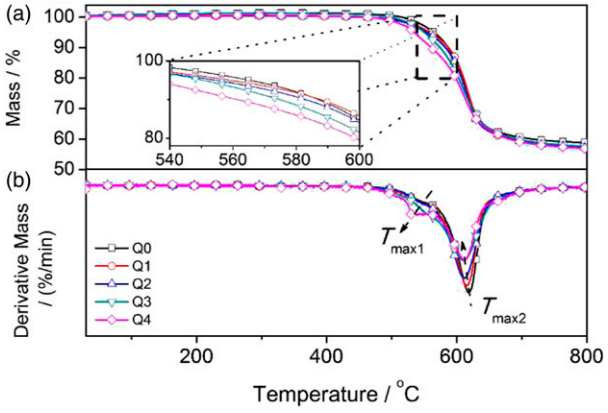

Figure 4. TGA (a) and DTG (b) curves of Co-PI films with various contents of DAA.

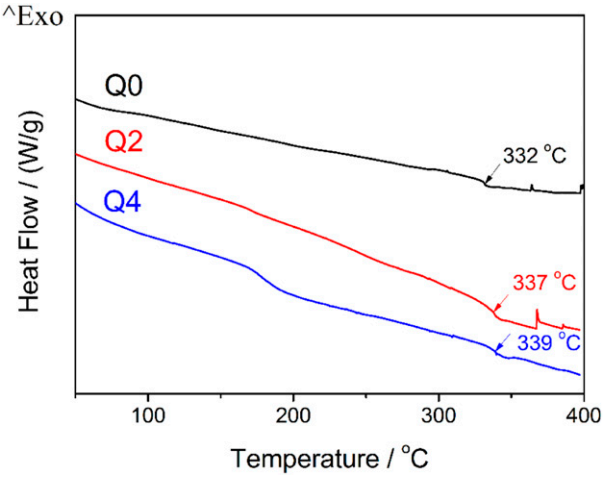

Figure 5. DSC curves of Co-PI films with various contents of DAA.

Thermal properties of Co-PI films

Thermal stability is also important for transparent and colorless PIs in terms of their applications on photoelectric devices. To investigate the effect of DAA introduction on

Table 3. Thermal and mechanical properties of Co-PI films.

Co-PI	T_5 /°C	T_{10} /°C	R /%	T_g/°C		CTE/(ppm/°C)	Tensile strength /MPa	Young's modulus /GPa	Elongation at break /%
				DMA[a]	DSC	30–200°C			
Q0	565	587	58.9	362	332	54.3	166.7 ± 1.8	2.3 ± 0.3	12.9 ± 2.0
Q1	559	588	57.3	366	335	53.5	158.9 ± 2.3	2.6 ± 0.4	11.6 ± 1.4
Q2	555	583	57.3	370	337	52.7	153.0 ± 0.7	3.7 ± 0.2	9.4 ± 0.3
Q3	551	575	57.6	374	338	50.7	145.2 ± 1.2	4.2 ± 0.6	8.2 ± 0.6
Q4	537	571	57.3	379	339	55.2	136.9 ± 0.9	5.1 ± 0.5	4.5 ± 1.2
Q5	535	561	57.0	/[b]	341	58.7	/[b]	/[b]	/[b]

[a]: the T_g is obtained from the tan δ peak temperature.
[b]: the film is too brittle to test.

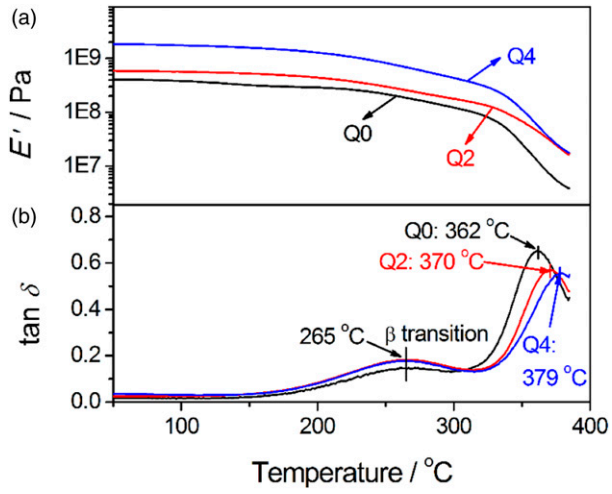

Figure 6. Storage modulus (*E*′, a) and tan δ (b) of Co-PI films with various contents of DAA.

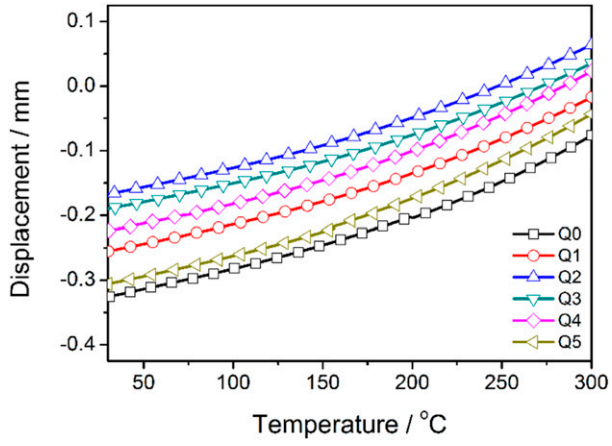

Figure 7. TMA curves of Co-PI films with various contents of DAA.

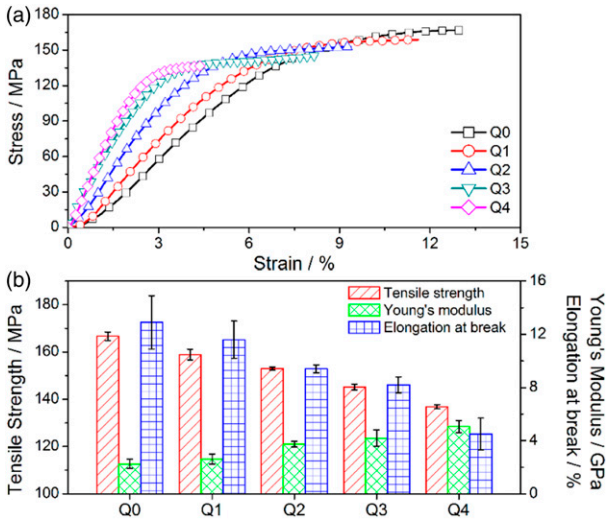

Figure 8. (a) Tensile stress-strain curves and (b) Tensile strength, Young's Modulus, and elongation at break of Co-PI films with various contents of DAA.

the thermal stability of the Co-PI films, thermogravimetric analysis (TGA) was used to characterize the thermal stability of the Co-PI films, and the TGA and DTG curves were plotted as shown in Figures 4(a) and (b), respectively. No obvious weight loss below 500°C in the TGA curves (Figure 4(a)) further indicated that all of the Co-PI films were completely imidized.[62,63] The 5% and 10% thermal weight loss temperatures (T_5 and T_{10}), residual yield (R%) at 800°C of the Co-PI films were listed in Table 3. All the copolyimides exhibited good thermal stability with the T_5 and T_{10} in the range of 530–565°C and 560–590°C. In addition, the R% is also slightly decreased with the loading of DAA. With the increasing content of alicyclic diamine (DAA), the content of aromatic structure in the Co-PI was decreased simultaneously. Compared with the aromatic structure, the alicyclic structure is easier to decompose under the condition of heating. As a result, the T_5, T_{10} and R% value decreased as the concentration of DAA increased. The detailed decomposition is revealed by the DTG curves (Figure 4(b)). Two peaks in the range of 480–560°C and 560–660°C representing the degradation of alicyclic and aromatic structure respectively,[63,64] existed in both DTG curves. With the increasing content of DAA, the intensity of the first peak increased and that of the second peak decreased. In addition, both the temperatures of first peak (T_{max1}) and second peak (T_{max2}) shift to the direction of low temperatures with the introduction of DAA.

The DSC curves of PIs are presented in Figure 5 and the corresponding T_g values were summarized in Table 3. The T_g of the Co-PI films is in the range 333–341°C and it increases with increasing molar content of adamantyl groups.

DMA was carried out to assess the mechanical characteristics of Co-PI films within the temperature range of 50–400°C. Figure 6 shows the temperature dependency of storage modulus (E') curve and tan δ of Co-PI films in nitrogen atmosphere. It is clearly shown that the E' is enhanced by the incorporation of DAA in the E'-temperature spectra. Two peaks were seen in the tan δ results of the Co-PI film with increased temperature. The first peak at approximately 265°C for Co-PI film corresponded to β transition and was attributed to the restricted rotational motion around the biphenyl components of the TFMB diamine moieties in the PI main chains.[65] The second peak temperature in tan δ curves was regarded as T_g, which was caused by the movement of the segments of the molecular chain. All the T_gs of the resulting Co-PIs were higher than 360°C. The T_gs obtained by DMA were slightly higher than

those by DSC, and the T_g obviously increased with increased DAA content. The relatively large bulky adamantane structure in the DAA unit and the -CF_3 of TFMB inhibit the free rotation of the polymer segments and block the movement of the copolymer chains, which may be the factor for the higher T_g value of these adamantane-based copolyimides.[66–68]

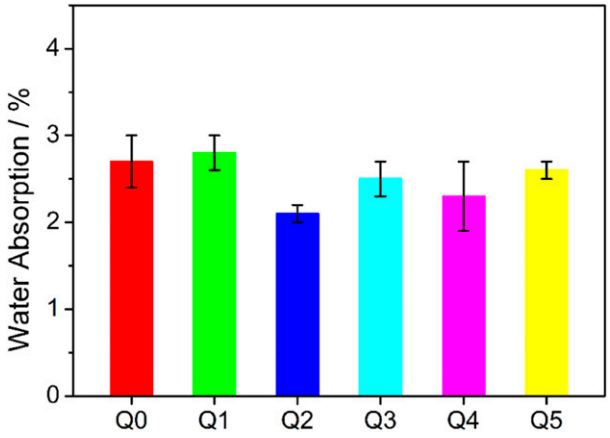

Figure 9. Water absorption of Co-PI films.

Table 4. Solubility of Co-PI films.

Co-PI	NMP	DMF	DMAc	DMSO	THF	Acetone	CH_2Cl_2
Q0	-	Δ	-	-	-	-	Δ
Q1	-	±	±	-	-	-	Δ
Q2	-	±	±	-	-	Δ	Δ
Q3	-	+	±	-	-	Δ	Δ
Q4	-	+	+	-	-	Δ	Δ
Q5	-	+	+	-	-	Δ	Δ

Completely soluble (+), partially soluble (±), swelling (Δ), and insoluble (−).

The dimensional stability of the Co-PI films was evaluated by thermomechanical analysis (TMA) measurements and the curves were outlined in Figure 7. It was observed that all the Co-PI films displayed a similar dimension change with the temperature increasing, and the CTE values obtained from these TMA curves were tabulated in Table 3. With the addition of DAA from 0 (Q0) to 1.30% (Q3), the CTE values in the range of 30–200°C and 100–200°C decreased from 54.3 to 50.7 ppm/°C and from 59.3 to 56.3 ppm/°C, respectively. This is because that a small amount of DAA can increase the rigidity of PI molecular chain.[42] However, the CTE values of Co-PI films rose again when the amount of DAA was more than 1.30% (Q4-Q5). This is caused by the excess of bulky adamantane groups in the polymer chains, which inhibit close packing and chain-chain interactions, thereby increasing the CTE.[69]

Mechanical properties of Co-PI films

Tensile measurements on Co-PI films were done and their stress-strain curves are presented in Figure 8(a). The Co-PI films have tensile strength of 136.9–166.7 MPa, Young's modulus of 2.25–5.06 GPa and elongation at break of 4.5–12.9%. These data are also summarized in Table 3 and plotted in Figure 8(b). Except for Q5 film which was too brittle to the test, the Co-PI films (Q0-Q4) showed decreased tensile strength and elongation at break with increasing molar ratio of adamantyl groups, while the Young's modulus increased correspondingly. This is probably because that the introduction of adamantane increases the rigidity of polymer chains and destroys the packing and entanglement of polymer chains. The mechanical properties of the films can be controlled by varying the molar ratio of DAA to TFMB.

Water absorption and organosolubility of Co-PI films

The water absorptions of the Co-PI films were in the range of 2.1–2.8%, as shown in Figure 9. The low water absorption of the copolymers is attributed to the hydrophobicity of the adamantyl and trifluoromethyl groups.

The solubility behavior of the Co-PI films in some solvents was listed in Table 4. It is observed that Q0 without DAA could not be dissolved or only be swelled in most known organic solvents. In sharp contrast, the adamantane-based Co-PI films (Q1-Q5) were completely or partially soluble in the aprotic polar solvents such as DMF and DMAc. The good solubility of the Co-PI films could be attributed to the introduction of the bulky adamantyl and trifluoromethyl groups, which disturb the close packing of the PI chains and lead to the increased free volume. Therefore, it will become easy for solvents to solubilize the polymers.

Conclusions

A series of Co-PI films with different mole ratios of TFMB/DAA were successfully obtained by copolymerizing of 6FDA, BPDA, TFMB and DAA through one-pot solution polycondensation and the relationship between the polymer components and their properties was investigated. Incorporation of DAA into polyimide improves the optical transparency and T_g of the resulting polyimides. Meanwhile, the drawback of high CTE value of fluorinated polyimide was compensated with increasing DAA content. These transparent co-polyimide films possess good solubility in most organic solvents, high T_g (T_g~362–379°C) and excellent optical properties (T_{430} > 80%). The existence of CF_3 groups and alicyclic structure loosens the PI chain stacking and breaks the conjugative effect of the main chain, thereby reducing the inter- and intramolecular CT interactions, which results in a decrease of film coloration and increase of solubility. Among the obtained

co-polyimides, Q3 shows best overall performance with high transmittance and T_g. In summary, this work provides a practical approach to develop high-performance transparent PI films with a combination of good solubility, high thermal stability and excellent optical properties, which exhibits great potential in the applications of substrates for optoelectronic engineering.

Declaration of Conflicting Interests

The author(s) declared no potential conflicts of interest with respect to the research, authorship, and/or publication of this article.

Funding

The author(s) disclosed receipt of the following financial support for the research, authorship, and/or publication of this article: This study is supported by the Jiaxing Science and Technology Bureau (2019AY11012), the ministry of science and technology(G2021013001 L) Shanghai Municipal Science and Technology Commission (19640770300), Engineering Research Center of Material Composition and Advanced Dispersion Technology, Ministry of Education, and Shanghai Municipal Education Commission.

ORCID iD

Qi Li https://orcid.org/0000-0002-2261-8659

References

1. Ji D, Li T, Hu W, et al. Recent progress in aromatic polyimide dielectrics for organic electronic devices and circuits. *Adv Mater* 2019; **31**: 1806070.
2. Yang SY (ed). *Advanced polyimide materials: Synthesis, characterization, and applications*. Amsterdam, the Netherlands: Elsevier BV; 2018.
3. Sanaeepur H, Amooghin AE, Bandehali S, et al. Polyimides in membrane gas separation: monomer's molecular design and structural engineering. *Prog Polym Sci* 2019; **91**: 80–125.
4. Ma P, Dai C, Wang H, et al. A review on high temperature resistant polyimide films: Heterocyclic structures and nanocomposites. *Compos Commun* 2019; **16**: 84–93.
5. Diaham S (ed). *Polyimide for electronic and electrical engineering applications*. London, UK: Intech Open Access Publisher; 2021.
6. Gouzman I, Grossman E, Verker R, et al. Advances in polyimide-based materials for space applications. *Adv Mater* 2019; **31**: 1807738.
7. Hicyilmaz AS and Bedeloglu AC. Applications of polyimide coatings: a review. *SN Appl Sci* 2021; **3**: 1–22.
8. Ree M. High performance polyimides for applications in microelectronics and flat panel displays. *Macromol Res* 2006; **14**: 1–33.
9. Kotov BV, GordinaVoishchev TA, et al. Aromatic polyimides as charge transfer complexes. *Polym Sci U.S.S.R* 1977; **19**: 711–716.
10. Dine-Hart RA and Wright WW. A study of some properties of aromatic imides. *Die Makromol Chemie: Macromol Chem Phys* 1971; **143**: 189–206.
11. Ando S, Matsuura T and Sasaki S. Coloration of aromatic polyimides and electronic properties of their source materials. *Polym J* 1997; **29**: 69–76.
12. Wozniak AI, Yegorov AS, Ivanov VS, et al. Recent progress in synthesis of fluorine containing monomers for polyimides. *J Fluorine Chem* 2015; **180**: 45–54.
13. Liu B, Hu W, Matsumoto T, et al. Synthesis and characterization of organosoluble ditrifluoromethylated aromatic polyimides. *J Polym Sci A: Polym Chem* 2005; **43**: 3018–3029.
14. Ando S, Matsuura T and Sasaki S. Perfluorinated polyimide synthesis. *Macromolecules* 1992; **25**: 5858–5860.
15. Shen J, Li X, Zhang Y, et al. Synthesis and characterization of highly soluble and optically transparent polyimides derived from novel fluorinated pyridine-containing aromatic diamine. *High Perform Polym* 2013; **25**: 268–277.
16. Tao L, Yang H, Liu J, et al. Synthesis and characterization of highly optical transparent and low dielectric constant fluorinated polyimides. *Polymer* 2009; **50**: 6009–6018.
17. Liu J, Nakamura Y, Suzuki Y, et al. Highly refractive and transparent polyimides derived from 4,4′-[*m*-sulfonylbis(phenylenesulfanyl)]diphthalic anhydride and various sulfur-containing aromatic diamines. *Macromolecules* 2007; **40**: 7902–7909.
18. Jia M, Li Y, He C, et al. Soluble perfluorocyclobutyl aryl ether-based polyimide for high-performance dielectric material. *ACS Appl Mater Inter* 2016; **8**: 26352–26358.
19. Lian R, Lei X, Xiao Y, et al. Synthesis and properties of colorless copolyimides derived from 4,4′-diaminodiphenyl ether-based diamines with different substituents. *Polym Chem* 2021; **12**: 4803–4811.
20. Yang CP, Chen YC, Hsiao SH, et al. Optically transparent and colorless poly(ether-imide)s derived from a phenylhydroquinone bis(ether anhydride) and various trifluoromethyl-substituted bis(ether amine)s. *J Polym Res* 2010; **17**: 779–788.
21. Zhou Y, Chen G, Wang W, et al. Comparative study of transparent polyimides derived from bis(ether anhydride)s and bis(ester anhydride)s using 2,2′-bis (trifluoromethyl) biphenyl-4,4′-diamine[J]. *High Perform Polym* 2017; **29**: 218–226.
22. Zhuang Y, Seong JG and Lee YM. Polyimides containing aliphatic/alicyclic segments in the main chains. *Prog Polym Sci* 2019; **92**: 35–88.
23. Mathews AS, Kim I and Ha CS. Synthesis, characterization, and properties of fully aliphatic polyimides and their derivatives for microelectronics and optoelectronics applications. *Macromol Res* 2007; **15**: 114–128.

24. Watanabe Y, Sakai Y, Shibasaki Y, et al. Synthesis of wholly alicyclic polyimides from N-silylated alicyclic diamines and alicyclic dianhydrides. *Macromolecules* 2002; **35**: 2277–2281.
25. Tapaswi PK, Choi MC, Jung YS, et al. Synthesis and characterization of fully aliphatic polyimides from an aliphatic dianhydride with piperazine spacer for enhanced solubility, transparency, and low dielectric constant. *J Polym Sci Part A: Polym Chem* 2014; **52**: 2316–2328.
26. Chen CK, Lin YC, Hsu LC, et al. High performance biomass-based polyimides for flexible electronic applications. *ACS Sustain Chem Eng* 2021; **9**: 3278–3288.
27. Dal Kim S, Lee S, Heo J, et al. Soluble polyimides with trifluoromethyl pendent groups. *Polymer* 2013; **54**: 5648–5654.
28. Bu Q, Zhang S, Li H, et al. Preparation and properties of thermally stable polyimides derived from asymmetric trifluoromethylated aromatic diamines and various dianhydrides. *Polym Degrad Stabil* 2011; **96**: 1911–1918.
29. Zuo HT, Gan F, Dong J, et al. Highly transparent and colorless polyimide film with low dielectric constant by introducing meta-substituted structure and trifluoromethyl groups. *Chin J. Polym. Sci* 2021; **39**: 455–464.
30. Xiao X, Qiu X, Kong D, et al. Optically transparent high temperature shape memory polymers. *Soft Matter* 2016; **12**: 2894–2900.
31. Wu Q, Ma X, Zheng F, et al. Synthesis of highly transparent and heat-resistant polyimides containing bulky pendant moieties. *Polym Int* 2019; **68**: 1186–1193.
32. Lu Y, Hao J, Xiao G, et al. Optical, thermal and gas separation properties of acetate-containing copoly(ether-imide)s based on 6FDA and fluorenyl diamines. *High Perform Polym* 2019; **31**: 1101–1111.
33. Li T, Huang H, Wang L, et al. High performance polyimides with good solubility and optical transparency formed by the introduction of alkyl and naphthalene groups into diamine monomers. *RSC Adv* 2017; **7**: 40996–41003.
34. Liu C, Pei X, Huang X, et al. Novel non-coplanar and tertbutyl-substituted polyimides: solubility, optical, thermal and dielectric properties. *Chin J. Chem* 2015; **33**(2): 277–284.
35. Hu X, Mu H, Wang Y, et al. Colorless polyimides derived from isomeric dicyclohexyl-tetracarboxylic dianhydrides for optoelectronic applications. *Polymer* 2018; **134**: 8–19.
36. Tapaswi PK and Ha CS. Recent trends on transparent colorless polyimides with balanced thermal and optical properties: design and synthesis. *Macromol Chem Phys* 2019; **220**: 1800313.
37. Ni H, Liu J, Wang Z, et al. A review on colorless and optically transparent polyimide films: chemistry, process and engineering applications. *J Ind Eng Chem* 2015; **28**: 16–27.
38. Matsuura T, Hasuda Y, Nishi S, et al. Polyimide derived from 2,2′-bis (trifluoromethyl)-4,4′-diaminobiphenyl. 1. Synthesis and characterization of polyimides prepared with 2,2′-bis(3,4-dicarboxyphenyl)hexafluoropropane dianhydride or pyromellitic dianhydride. *Macromolecules* 1991; **24**: 5001–5005.
39. Wu X, Cai J and Cheng Y. Synthesis and characterization of high fluorine-containing polyimides with low-dielectric constant. *J Appl Polym Sci* 2021: 51972.
40. Mathias LJ, Jensen JJ, Reichert VT, et al. Adamantane-containing polymers. In: Labadie JW, Hedrick JL, Ueda M, et al. (eds). *Step-growth polymers for high-performance materials. Am. Chem. Soc. Adv. Chem. Ser*, **624**. Washington, DC: American Chemical Society; 1996, pp. 197–207.
41. Lau ZR, Sin SL, Yan H, et al. Adamantane-modified polyurethanes: Effect of hydroxy group of adamantane on the properties of polyurethanes. *Adv Mater Res* 2015; **1110**: 92–95.
42. Tsai CW, Wu KH, Yang CC, et al. Adamantane-based epoxy resin and siloxane-modified adamantane-based epoxy resin: characterization of thermal, dielectric and optical properties. *React Funct Polym* 2015; **91**: 11–18.
43. Ishizone T and Goseki R. Synthesis of polymers carrying adamantyl substituents in side chain. *Polym J* 2018; **50**: 805–819.
44. Mathews AS, Kim I and Ha CS. Fully aliphatic polyimides from adamantane-based diamines for enhanced thermal stability, solubility, transparency, and low dielectric constant. *J Appl Polym Sci* 2006; **102**: 3316–3326.
45. Maya EM, Garcia-Yoldi I, Lozano AE, et al. Synthesis, characterization, and gas separation properties of novel copolyimides containing adamantyl ester pendant groups. *Macromolecules* 2011; **44**: 2780–2790.
46. Novakov IA, Orlinson BS, Zav'yalov DV, et al. Synthesis and properties of new transparent (co) polyimides based on adamantane-containing diamines and aromatic tetracarboxylic dianhydrides. *Russ Chem Bull* 2021; **70**: 1141–1148.
47. Hasegawa M.. Development of solution-processable, optically transparent polyimides with ultra-low linear coefficients of thermal expansion. *Polymers* 2017; **9**: 520.
48. Lv P, Dong Z, Dai X, et al. Flexible polydimethylsiloxane-based porous polyimide films with an ultralow dielectric constant and remarkable water resistance. *ACS Appl Polym Mater* 2019; **1**: 2597–2605.
49. Yi MH, Huang W, Lee BJ, et al. Synthesis and characterization of soluble polyimides from 2,2-bis(4-aminophenyl) cycloalkane derivatives. *J Polym Sci Part A: Polym Chem* 1999; **37**: 3449–3454.
50. Huang X, Li H, Liu C, et al. Design and synthesis of high heat-resistant, soluble, and hydrophobic fluorinated polyimides containing pyridine and trifluoromethylthiophenyl units. *High Perform Polym* 2019; **31**: 107–115.
51. Hsiao SH, Yang CP and Huang SC. Preparation and properties of new polyimides and polyamides based on 1,4-bis(4-amino-2-trifluoromethylphenoxy) naphthalene. *J Polym Sci A: Poly Chem* 2004; **42**: 2377–2394.
52. Zhang Y, Qu L, Liu J, et al. Synthesis and characterization of high-temperature-resistant and optically transparent polyimide coatings for potential applications in quartz

optical fibers protection. *J Coat Technol Res* 2019; **16**: 511–520.
53. Wang X, Zhang P, Chen Y, et al. Characterization of alignment correlation between LC molecules and chemical groups on/in the surface of polyimide films with biphenyl side chains. *Macromolecules* 2011; **44**: 9731–9737.
54. Geng Z, Lu Y, Zhang S, et al. Synthesis and characterization of novel adamantane-based copoly(aryl ether ketone)s with low dielectric constants. *Polym Int* 2014; **63**(2): 333–337.
55. Lv P, Dong Z, Dai X, et al. Synthesis and properties of ultralow dielectric porous polyimide films containing adamantane. *J Polym Sci Part A: Polym Chem* 2018; **56**(5): 549–559.
56. Liu H, Zhai L, Bai L, et al. Synthesis and characterization of optically transparent semi-aromatic polyimide films with low fluorine content. *Polymer* 2019; **163**: 106–114.
57. Zhang M, Liu W, Gao X, et al. Preparation and characterization of semi-alicyclic polyimides containing trifluoromethyl groups for optoelectronic application. *Polymers* 2020; **12**: 1532.
58. Yu HC, Jung JW, Choi JY, et al. Structure-property relationship study of partially aliphatic copolyimides for preparation of flexible and transparent polyimide films. *J Macromol Sci A* 2017; **54**: 97–104.
59. Jeong HY, Lee YK, Talaie A, et al. Synthesis and characterization of the first adamantane-based poly(*p*-phenylenevinylene) derivative: An intelligent plastic for smart electronic displays. *Thin Solid Films* 2002; **417**(1–2): 171–174.
60. Mittal KL. *Polyimides and other high temperature polymers: Synthesis, characterization and applications*, **Volume 3**. Boca Raton, FL: Taylor & Francis Group, LLC, 2005, pp. 69–88.
61. Yu XH, Liu JN and Wu DY. Colorless PI structure design and evaluation for achieving low CTE target. *Mater Today Com* 2019; **21**: 100562.
62. Wu Z, Han B, Zhang C, et al. Novel soluble and optically active polyimides containing axially asymmetric 9,9′-spirobifluorene units: synthesis, thermal, optical and chiral properties. *Polymer* 2012; **53**: 5706–5716.
63. Kim JC and Chang JH. Quaternary copolyimides with various monomer contents: Thermal property and optical transparency. *Macromol Res* 2014; **22**: 1178–1182.
64. Lan Z, Li C, Yu Y, et al. Colorless semi-alicyclic copolyimides with high thermal stability and solubility. *Polymers* 2019; **11**: 1319.
65. Ando S, Sekiguchi K, Mizoroki M, et al. Anisotropic linear and volumetric thermal-expansion behaviors of self-standing polyimide films analyzed by thermomechanical analysis (TMA) and optical interferometry. *Macromol Chem Phys* 2018; **219**(3): 1700354.
66. Lao H, Mushtaq N, Chen G, et al. Transparent polyamide-imide films with high T_g and low coefficient of thermal expansion: Design and synthesis. *Polymer* 2020; **206**: 122889.
67. Wang G, Geng Z, Zhu X, et al. Synthesis and characterization of soluble low-κ poly(aryl ether ketone) copolymers with pendent adamantyl groups. *High Perform Polym* 2010; **22**: 779–798.
68. Yi L, Li C, Huang W, et al. Soluble and transparent polyimides with high T_g from a new diamine containing tert-butyl and fluorene units. *J Polym Sci Part A: Polym Chem* 2016; **54**(7): 976–984.
69. Miao J, Hu X, Wang X, et al. Colorless polyimides derived from adamantane-containing diamines. *Polym Chem* 2020; **11**: 6009–6016.